Evidence of non-statistical neutron emission following β-decay near doubly magic ^{132}Sn

J. Heideman,[1] R. Grzywacz,[1,2] Z. Y. Xu,[1] M. Madurga,[1] J. E. Escher,[3] T. Kawano,[4] A. Algora,[5,6]
A. N. Andreyev,[7,8] J. Benito,[9] T. Berry,[10] M. J. G. Borge,[11] C. Costache,[12] H. De Witte,[13] A. Fijalkowska,[14,15]
L. M. Fraile,[9] H. O. U. Fynbo,[16] A. Gottardo,[17] C. Halverson,[1] L. J. Harkness-Brennan,[18] A. Illana,[13,19]
Ł. Janiak,[14,20] D. S. Judson,[18] T. T. King,[1] A. Korgul,[14] T. Kurtukian-Nieto,[21] I. Lazarus,[22] R. Lică,[23,12]
R. Lozeva,[24] N. Marginean,[12] R. Marginean,[12] C. Mazzocchi,[14] C. Mihai,[12] R. E. Mihai,[12] A.I. Morales,[5]
R.D. Page,[18] J. Pakarinen,[19,25] M. Piersa-Siłkowska,[14] Zs. Podolyák,[10] M. Singh,[1] C. Sotty,[12] M. Stepaniuk,[14]
O. Tengblad,[11] A. Turturica,[12] P. Van Duppen,[13] V. Vedia,[9] S. Viñals,[11] N. Warr,[26] R. Yokoyama,[1] and C. X. Yuan[27]

(IDS Collaboration)

[1]*Department of Physics and Astronomy, University of Tennessee, Knoxville, Tennessee 37996, USA*
[2]*Physics Division, Oak Ridge National Laboratory, Oak Ridge, Tennessee 37831, USA*
[3]*Nuclear and Chemical Sciences Division, Lawrence Livermore National Laboratory, Livermore, California 94551, USA*
[4]*Theoretical Division, Los Alamos National Lab, Los Alamos, New Mexico 87545, USA*
[5]*Instituto de Física Corpuscular, CSIC-Universidad de Valencia, E-46071, Valencia, Spain*
[6]*Institute for Nuclear Research (ATOMKI), H-4026 Debrecen, Bem tér 18/c, Hungary*
[7]*University of York, Department of Physics, York YO10 5DD, North Yorkshire, United Kingdom*
[8]*Advanced Science Research Center (ASRC), Japan Atomic Energy Agency (JAEA), Tokai-mura, Japan*
[9]*Grupo de Física Nuclear and IPARCOS, Universidad Complutense de Madrid, CEI Moncloa, E-28040 Madrid, Spain*
[10]*Department of Physics, University of Surrey, Guildford GU2 7XH, United Kingdom*
[11]*Instituto de Estructura de la Materia, IEM-CSIC, Serrano 123, E-28006 Madrid, Spain*
[12]*Horia Hulubei National Institute for Physics and Nuclear Engineering, RO-077125 Bucharest, Romania*
[13]*KU Leuven, Instituut voor Kern- en Stralingsfysica, B-3001 Leuven, Belgium*
[14]*Faculty of Physics, University of Warsaw, PL 02-093 Warsaw, Poland*
[15]*Department of Physics and Astronomy, Rutgers University, New Brunswick, New Jersey 08903, USA*
[16]*Department of Physics and Astronomy, Aarhus University, DK-8000 Aarhus C, Denmark*
[17]*IPN, IN2P3-CNRS, Université Paris-Sud, Université Paris Saclay, 91406 Orsay Cedex, France*
[18]*Department of Physics, Oliver Lodge Laboratory,*
University of Liverpool, Liverpool L69 7ZE, United Kingdom
[19]*University of Jyväskylä, Department of Physics, P.O. Box 35, FI-40014, Jyväskylä, Finland*
[20]*National Centre for Nuclear Research, 05-400 Otwock, Świerk, Poland*
[21]*CENBG, Université de Bordeaux—UMR 5797 CNRS/IN2P3, Chemin du Solarium, 33175 Gradignan, France*
[22]*STFC Daresbury, Daresbury, Warrington WA4 4AD, United Kingdom*
[23]*ISOLDE, EP Department, CERN, CH-1211 Geneva, Switzerland*
[24]*Univeristé Paris-Saclay, IJCLab, CNRS/IN2P3, F-91405 Orsay, France*
[25]*Helsinki Institute of Physics, University of Helsinki, P.O. Box 64, FIN-00014, Helsinki, Finland*
[26]*Institut für Kernphysik, Universität zu Köln, 50937 Köln, Germany*
[27]*Sino-French Institute of Nuclear Engineering and Technology,*
Sun Yat-Sen University, Zhuhai, 519082, Guangdong, China
(Dated: May 28, 2023)

Models of the β-delayed neutron emission (βn) assume that neutrons are emitted statistically via an intermediate compound nucleus post β decay. Evidence to the contrary was found in an ^{134}In β-decay experiment carried out at ISOLDE CERN. Neutron emission probabilities from the unbound states in ^{134}Sn to known low-lying, single-particle states in ^{133}Sn were measured. The neutron energies were determined using the time-of-flight technique, and the subsequent decay of excited states in ^{133}Sn was studied using γ-ray detectors. Individual βn probabilities were determined by correlating the relative intensities and energies of neutrons and γ rays. The experimental data disagree with the predictions of representative statistical models which are based upon the compound nucleus postulate. Our results suggest that violation of the compound nucleus assumption may occur in β-delayed neutron emission. This impacts the neutron-emission probabilities and other properties of nuclei participating in the r-process. A model of neutron emission, which links the observed neutron emission probabilities to nuclear shell effects, is proposed.

I. INTRODUCTION

Modern models of β-delayed neutron emission (βn) separate the process into two stages [1], starting with the β decay of a parent nucleus followed by the neutron emission from the unbound daughter states. The first step is mediated by the weak interaction and requires knowledge of the β-decay strength function feeding neu-

tron unbound states [2, 3]. This stage is very sensitive to nuclear-structure details. In the second step, the Bohr compound nucleus (CN) hypothesis is asserted for neutron emission [2, 4, 5], i.e., the CN is assumed to have a large density of levels and no memory of specific configurations populated in β decay besides the inherited spin and parity (J^{π}) [4, 6]. Neutron emission is considered a statistical process which depends upon the excitation energy, spin, and angular momentum of the CN and on available states in the residual nucleus [2, 6]. Although statistical neutron-emission models have successfully described gross properties of βn process in some medium- and heavy-mass nuclei [2, 3, 7], they have yet to be tested against neutron and γ-ray spectra for broader sets of isotopes. Accurate predictions of βn precursor behavior, such as βn probabilities (P_n), are essential for the rapid neutron-capture process (r-process) calculations, especially in astrophysical environments where β decay competes with neutron capture [8]. Verifications of pre-existing βn models are needed to reliably model r-process nucleosynthesis.

The purely statistical nature of βn was questioned previously based on the early observation of discrete neutron energy distributions [9, 10]. Hardy *et al.* interpreted these features to be purely statistical and due to the level density fluctuations in the β-decay daughter [5, 11]. Modern shell-model calculations can capture the complexity of β-decay feeding patterns, reproducing the observed discrete neutron spectra, thus establishing a direct link to nuclear structure. However, the universal applicability of the statistical approach to describe neutron emission from the states selectively populated in β decay remains an open question. Nuclei in the vicinity of doubly magic ^{132}Sn are unique candidates to study the limits of neutron-emission models because conditions in these nuclei are different from mid-shell nuclei which are typically considered prototypical statistical β-delayed neutron emitters.

In this paper, the decay of ^{134}In is revisited to test the accuracy of statistical-model predictions. ^{134}In is a known β-delayed neutron emitter, predominantly populating neutron unbound states in ^{134}Sn [12, 13] via β decay. The ^{134}Sn states then decay via neutron emission to low-lying, single-particle states in ^{133}Sn [14]. The βn probability of ^{134}In is large, with P_{1n}=89(3)% and P_{2n}=9(2)% [13], due to the sizeable β-decay energy window, $Q_{\beta} = 14.5(2)$ MeV, and the small neutron separation energy of ^{134}Sn, $S_n = 3.62$ MeV [15, 16]. The ground-state spin and parity assignment of ^{134}In has previously been constrained to 6^- or 7^- [13]. With respect to the ^{132}Sn doubly magic core, the states populated in ^{134}Sn via allowed Gamow-Teller (GT) transitions consist predominately of particle-hole (p-h) configurations around 7-MeV excitation energy [13, 17, 18]. Schematics of the neutron occupation for ^{134}Sn and ^{133}Sn states of interest are shown in the diagram in the upper right of Fig. 1. Within the spherical shell-model framework, the ^{134}Sn neutron p-h states (Box 1 in Fig. 1) are orthogo-

nal to the ^{133}Sn neutron single-particle states (Box 3 in Fig. 1). By studying the neutron emissions from these ^{134}Sn states, the critical question of whether the Bohr hypothesis is applicable for every βn precursor can possibly be answered. If the β-decay daughter dampens into a structureless CN (Box 2.a in Fig. 1), neutron-emission calculations made with a Hauser-Feshbach model should accurately describe experimental data [2, 6]. This scenario is represented by the large yellow arrows in Fig. 1. An alternate scenario, indicated by the large green arrows in Fig. 1, involves direct neutron emission enabled by the minor wave function components (Box 2.b in Fig. 1) of the excited states. This could be evidenced by observing deviations from CN predictions. In this work, we combined neutron and γ-ray spectroscopy methods, measuring the relative population of states in ^{133}Sn through neutron emission from ^{134}Sn excited states. These results will be compared to predictions made assuming neutron emission from a CN.
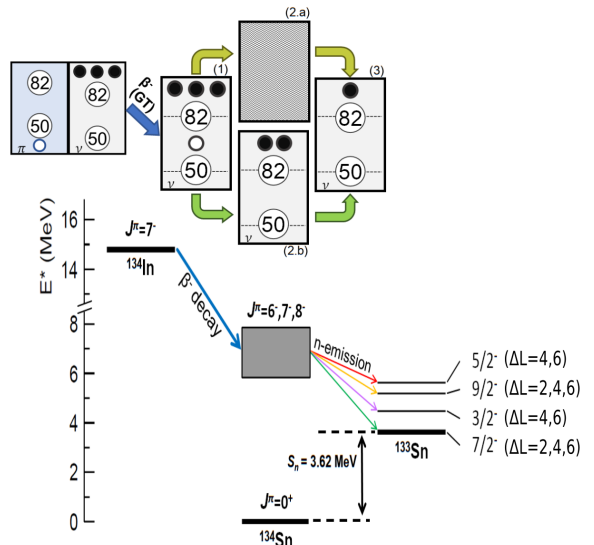

FIG. 1. Schematic of ^{134}In βn emission representing the β decay to neutron unbound states in ^{134}Sn and subsequent neutron emission to single-particle states in ^{133}Sn.ISOL As an example, the schematic is labeled assuming an initial ^{134}In $J^{\pi} = 7^-$. Two different scenarios for neutron emission, statistical neutron emission and direct neutron emission, are represented by boxes 2.a and 2.b respectively.

II. EXPERIMENTAL DETAILS

Radioactive nuclei were produced at the Isotope Separator On-Line (ISOLDE) facility at CERN using a 1.4 GeV proton beam incident on a uranium carbide (UC$_x$) target [19]. Indium nuclei were selectively ionized using the Resonance Ionization Laser Ion Source (RILIS) and then mass-separated by the General Purpose Separator (GPS) [20]. The ^{134}In ions were delivered to the

ISOLDE Decay Station (IDS) and implanted on a movable tape system for beta-decay measurement.

The tape system is operated in a take-away mode. At the start of a tape cycle, ions are continuously implanted on the tape for 300 ms while measuring decays before the beam was turned off. Decay measurements were made for another 300 ms before the tape was cycled a fixed amount to remove the long-lived contaminants. This created a 600 ms time window for observing ^{134}In decays. The IDS detector setup consists of one beta detector with dual photomultiplier tube (PMT) readout, four high-purity Ge (HPGe) clovers, and the IDS Neutron Detector (INDiE) [18], an array using the same concept as the Versatile Array of Neutron Detectors at Low Energy (VANDLE) [21]. The plastic scintillator beta detector serves to measure the beta energy from ^{134}In decay and provide a start signal associated with the neutron emission. The average efficiency for beta detection is $\sim 80\%$. The beta detector and tape system are all enclosed in an aluminum vacuum chamber. The four HPGe detectors have 10% and 3% total efficiency for 100 keV and 1 MeV gamma rays respectively without addback. INDiE consists of twenty-six bars of Eljen 200 plastic scintillator, each 3x6x120 cm^3, which measure neutron times-of-flight. The bars are arranged in a cylindrical arc on an aluminum frame 104 cm from the implant point, covering 11.7% of a 4π solid angle. Due to shadowing from a steel support frame, four detectors were not used in this analysis, reducing the solid angle coverage to 10%. INDiE is placed on the opposite side of the implant point from the HPGe detectors to minimize the interactions of neutrons emitted towards INDiE. Each end of a scintillator detector is coupled to a PMT, and each detector is gain matched to ensure a consistent response to neutrons with the same energy across all of INDiE.

All β-, γ-, and neutron-detector signals were connected to a digital data acquisition (DDAQ). The details of the DDAQ system are described in Ref. [22]. The 250-MHz digitized waveforms (4-ns period) were recorded for the signals from the two β detectors and 26 INDiE modules, while only the energy filter samplings were stored for the HPGe signals. Waveforms were then analyzed offline to extract a high-resolution timestamp (HRT). This technique achieves timing resolutions below the digitizer sampling period. Using a polynomial constant fraction discriminator (polyCFD) algorithm [23], HRTs are calculated to measure the time difference between β and neutron signals. The FWHM resolution of the γ-flash peak in the TOF histogram such obtained is 1.5 ns. Well-known ^{17}N β-delayed neutron-emission data [24] were used to calibrate the individual distances from the implant position to each INDiE bar. The average distance to the center of each bar in this setup is 104.2(3) cm.

The ^{134}Cs isomer contamination caused significant background in all detector systems. The isomer half-life is 2.9 hours and predominately decays via a 127.5-keV γ ray. The large number of γ rays detected by the β detector caused significant, non-constant background in
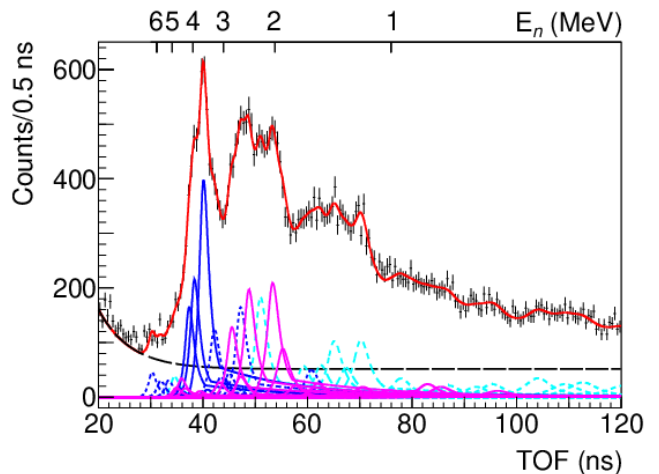

FIG. 2. Full TOF spectrum with analytical deconvolution given by red line with the underlying γ-ray background represented by the dashed black line. Individual neutron transitions are represented by the underlying curves. Color and dash schemes are related to the analysis process. The ground state neutron-emissions are marked with dark blue. Components of the ^{133}Sn excited states are plotted in magenta. Additional responses are marked in light blue. See text for additional details.

the neutron TOF spectrum. This behavior was removed by requiring the amplitude of β signals to be above the equivalent light output of 127.5 keV$_{ee}$. For INDiE detectors, the beam contamination caused a constant flat background, mainly by low-energy signals, in the neutron TOF spectrum. No requirement on the amplitude of neutron signals was made due to the low overall contribution of this effect to the shape of the spectrum and the possibility of removing low-energy neutron events.

III. DATA ANALYSIS

A fully corrected neutron TOF spectrum showing the main region of interest is plotted in Fig. 2. The γ-ray energy spectra following β-decay (black) and βn (red) events are shown in Fig. 3 (top) Three γ-ray transitions associated with the deexcitation of the neutron single-particle states in ^{133}Sn ($3/2^-$ at 854 keV, $9/2^-$ at 1561 keV, and $5/2^-$ at 2004 keV [12, 14]) are indicated by blue arrows. The spectrum reflects the complexity of neutron emission from ^{134}Sn due to the low-lying states in ^{133}Sn that can be fed by neutron emission and vary the neutron energies in the βn process. It also shows the effects of neutron interactions with materials of the experimental system before being detected. In Geant4 [25], mono-energetic neutrons are emitted isotropically from the ion implantation point to generate TOF histograms which include these scattering effects. Each TOF distribution has two main features, a prompt peak centered near the nominal neutron TOF, and a long tail which can carry on for hundreds of nanoseconds. A piecewise response

function, represented by an asymmetric Lorentzian followed by three sequential exponential decay tails, is used to characterize each histogram. From fits to each simulation of different monoenergetic neutrons, a neutron response function is generated by finding the relationship between each parameter and the associated neutron energies. The response function is verified by properly deconvolving well-known ^{17}N [24] and ^{49}K [26] β-delayed neutron spectra.
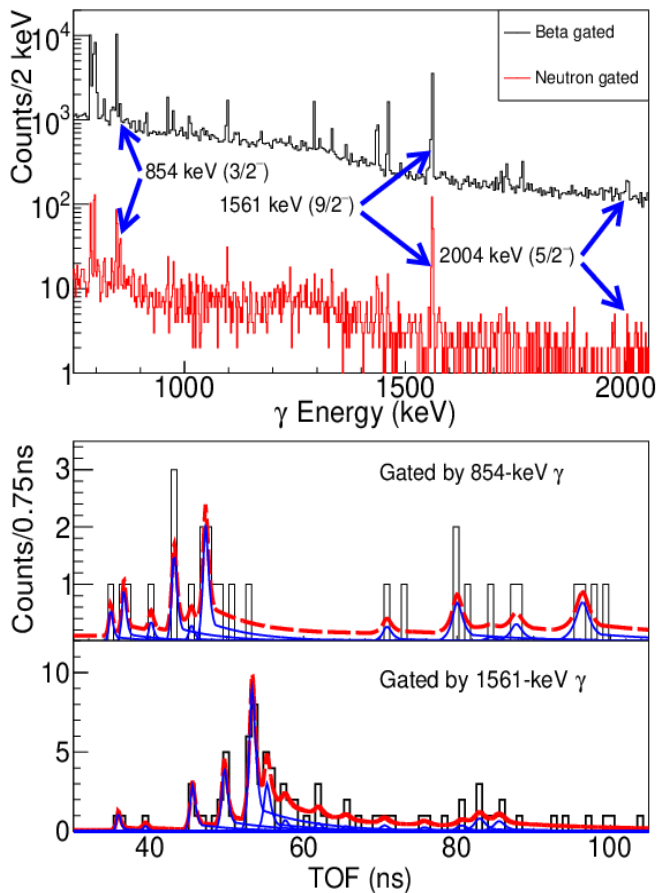

FIG. 3. Gamma-ray energies observed following a beta decay event (top). Neutron time-of-flight distribution in coincidence with the 854- (middle) and 1561-keV (bottom) γ rays, which correspond to the deexcitations from the $3/2^-$ and $9/2^-$ excited states to the $7/2^-$ ground state in ^{133}Sn, respectively.

To start deconvolving the neutron TOF spectrum in Fig. 2, additional neutron TOF spectra gated by the γ rays deexciting the $3/2^-$ (854 keV) and $9/2^-$ (1561 keV) states in ^{133}Sn, shown in Fig. 3 (bottom), were made to extract a ^{134}Sn preliminary level scheme. Due to the low neutron-emission branching ratio to the ^{133}Sn $5/2^-$ state combined with the short run time for this experiment, no valid neutron TOFs were measured in coincidence with 2004-keV γ rays. After establishing the initial set of ^{134}Sn levels which have a neutron-emission component to the ^{133}Sn excited states, those neutrons were included in the deconvolution process of the full spec-

trum in Fig. 2 (magenta) with fixed centroid positions established from neutron-gamma analysis. The amplitudes of those peaks were allowed to vary within 20% of their γ-efficiency corrected amplitudes. Then, neutron energies corresponding to the decay of these ^{134}Sn states to the ^{133}Sn ground state were calculated and included in the deconvolution at their respective TOF (dark blue). Amplitudes of those ground-state-feeding peaks were allowed to vary fully. For the states with strong neutron-γ cascade, the centroids of their ground-feeding peaks were fixed (solid dark blue). The rest had their centroids free to vary within the TOF uncertainty at that energy (dashed dark blue). While the preliminary neutron-γ information somewhat reproduced the TOF spectrum between 30 and 60 ns, there were deficiencies in the number of transitions for longer TOF not accounted for by neutron scattering effects. Additional responses (dashed light blue) were added where the spectrum was not properly described until the best χ^2/NDF of overall fit was achieved. The whole neutron response function sits on top of the γ-ray background, represented by a dashed black line in Fig. 2, which is characterized by a double exponential with a constant offset. The red line in Fig. 2 is the analytical deconvolution of the full neutron TOF spectrum which contains the aggregated sum of all individual neutron responses along with the γ ray background.

IV. RESULTS AND DISCUSSIONS

The key observables of this experiment are β feeding intensities, I_β, to ^{134}Sn neutron-emitting states and the subsequent neutron feeding intensities, $I_{\beta n_i}$, to the single-particle states in ^{133}Sn. $I_{\beta n_i}$ values were given by the area of individual neutron responses extracted from the deconvolution analysis seen in Fig. 2, which are then summed for each ^{134}Sn excitation energy to find I_β. Decay feeding to states in ^{134}Sn can be seen in Fig. 4(B), where a single level's shading represents $I_{\beta n_i}$. The most prominently populated excited states are concentrated near $E_x \sim 7$ MeV in the ^{134}Sn neutron-emitting nucleus. Comparative half-lives (log ft) values are calculated in order to determine each state's likelihood as having undergone a GT or first-forbidden (FF) transition. Only states populated in GT transitions are considered in the following discussions because they are exclusively assumed to only be neutron p-h configurations. Five states of interest were identified for studying neutron emission from states populated through a GT transition. Their energies are 6.88 MeV, 7.18 MeV, 7.37 MeV, 7.81 MeV, and 8.31 MeV, with the calculated log ft values 5.0(1), 4.9(1), 5.0(1), $5.3^{+0.3}_{-0.2}$, and $5.0^{+0.5}_{-0.3}$, respectively.
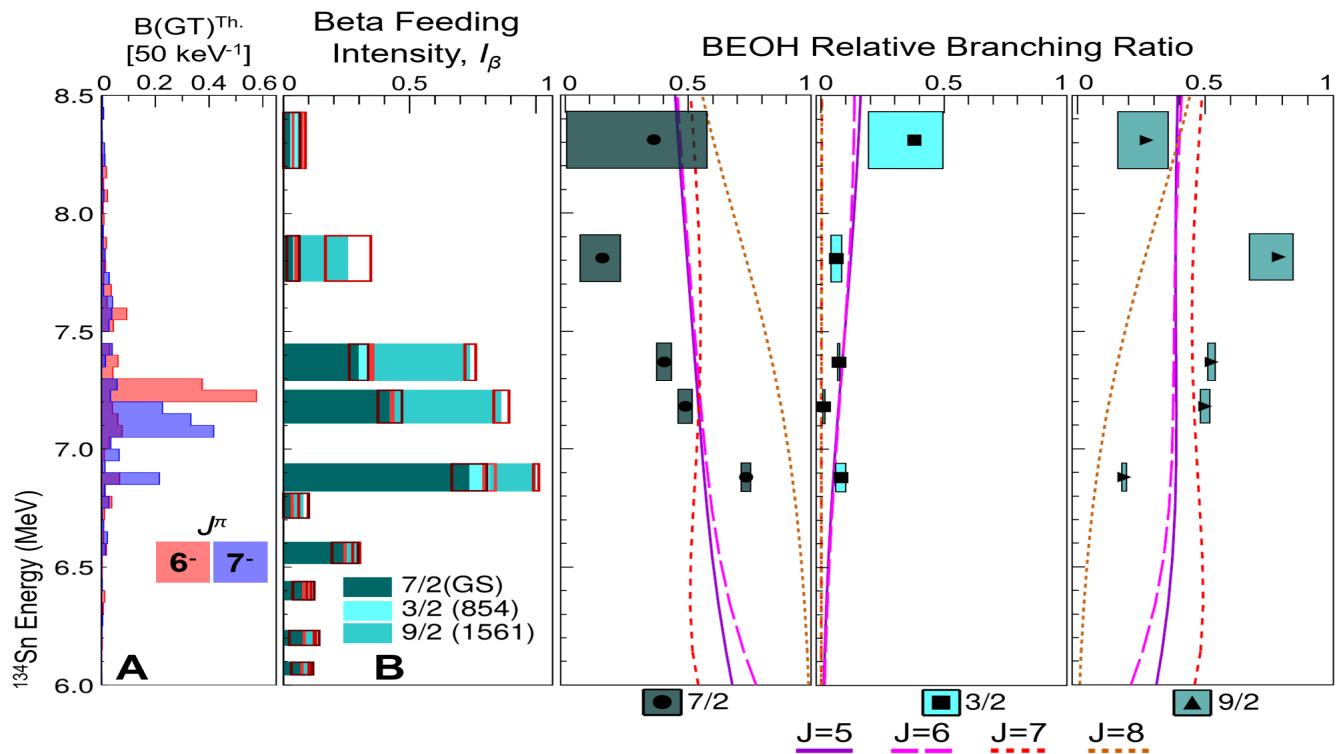
FIG. 4. A: Theoretical B(GT) values from LSSM calculations for $J^\pi = 6^-, 7^-$ ^{134}In ground state spin and parity. B: Measured feeding intensities to excited states in ^{133}Sn, I_β, where the largest intensity has been normalized to unity. Column shading represents $I_{\beta n_i}$. The red rectangles reflect the uncertainty in intensity and energy for each point. C, D, E: BeoH calculations of the relative neutron branching ratios to the $7/2^-$ (C), $3/2^-$ (D), and the $9/2^-$ (E) states in ^{133}Sn. Black data points in each panel are the experimentally determined neutron branching ratios.

A.   Shell-model calculations of β-decay strength

Large-scale shell-model (LSSM) calculations of β-decay strengths, including both GT and FF decays, in ^{134}Sn were carried out to support the hypothesis that these five states could be populated in GT transitions. The calculations were performed from 6^- and 7^- ^{134}In ground states according to suggested spin assignments [13]. It was presumed that, like in ^{133}In decay, the main GT transition from ^{134}In to ^{134}Sn would involve neutron p-h states in ^{134}Sn [17, 18]. To include these states, the valence space of LSSM was built around an ^{88}Sr core ($Z = 38$, $N = 50$). Orbitals $1p_{1/2}$, $0g_{9/2}$, $0g_{7/2}$, $1d_{5/2}$, $1d_{3/2}$, and $2s_{1/2}$ are included for valence protons and orbitals $0g_{7/2}$, $1d_{5/2}$, $1d_{3/2}$, $2s_{1/2}$, $0h_{11/2}$, and $1f_{7/2}$ are included for valence neutrons. Two body interactions are derived from a $V_{\rm MU}$ plus M3Y [27, 28] effective nucleon-nucleon potential. The GT and FF strengths were calculated using the respective operators defined in Ref. [29]. Strength distributions for GT transitions can be seen in Fig. 4(A). The GT strength distribution is relatively unchanged between the two ^{134}In calculations with 6^- and 7^- spin assumption and is consistent with the experimental observation in Fig. 4(B). The FF transitions are negligible compared to the GT in the region of interest at $E_x \sim 7$ MeV. While these calculations were performed to

provide an interpretation of the dominant transition, the configuration space was chosen to calculate p-h states. Most importantly only the $f_{7/2}$ neutron single particle level was included outside $N = 82$ closed core. This choice was forced by the computational feasibility of the LSSM calculations.

B.   Neutron emission from statistical model

Neutron emission branching ratios to the low-lying excited states in ^{133}Sn were calculated as a function of ^{134}Sn excitation energy and spins of either $J^\pi = 5^-, 6^-, 7^-$ for $J^\pi_{gs}(^{134}{\rm In}) = 6^-$, or $J^\pi = 6^-, 7^-, 8^-$ for $J^\pi_{gs}(^{134}{\rm In}) = 7^-$ using BeoH code [30] which predicts statistical neutron emission probabilities [2, 6]. BeoH calculates the neutron and γ emissions from a CN for given energy and J^π [30]. The Koning-Delaroche optical model [31] is used to calculate neutron transmission coefficients [2]. In order to account for non-observed decay branches, the total intensity of feeding per energy bin to the $7/2^-$, $3/2^-$, and $9/2^-$ states in BeoH calculations was normalized to one. The relative intensities feeding the $7/2^-$, $3/2^-$, and $9/2^-$ states are shown in Figs. 4(C), (D), and (E), respectively.

Experimental data representing the relative intensities from the five states of interest are overlaid in the corre-

sponding figures. If this statistical model accurately predicts the neutron-emission behavior, neutron branching ratios of each ^{134}Sn state of a given J^π should match closely between experimental data and the BeoH calculations. However, the experimental relative branching ratios are only consistent with BeoH calculations of the 7.18-MeV state, for which the strongest agreement is $J^\pi = 7^-$. For the rest of the states, even if the observed neutron transitions belong to an unresolved group of states with different spins, no mixture of spins with each group can reproduce the experimental data. Other levels could be made to agree with experimental results if contributions from $J^\pi = 9^-$ neutron-emitting states in ^{134}Sn were considered. However, this scenario is precluded by the $J^\pi_{gs}(^{134}\text{In}) = 6^-$ or 7^- assignment [13] and β-decay selection rules for allowed GT decays ($\Delta J = 0, \pm 1$). We attempted to resolve the differences between experimental data and theoretical calculations by considering an alternative optical model parameterization from Becchetti-Greenlees [32], which failed to show significant improvement over the other in comparison with the experiment.
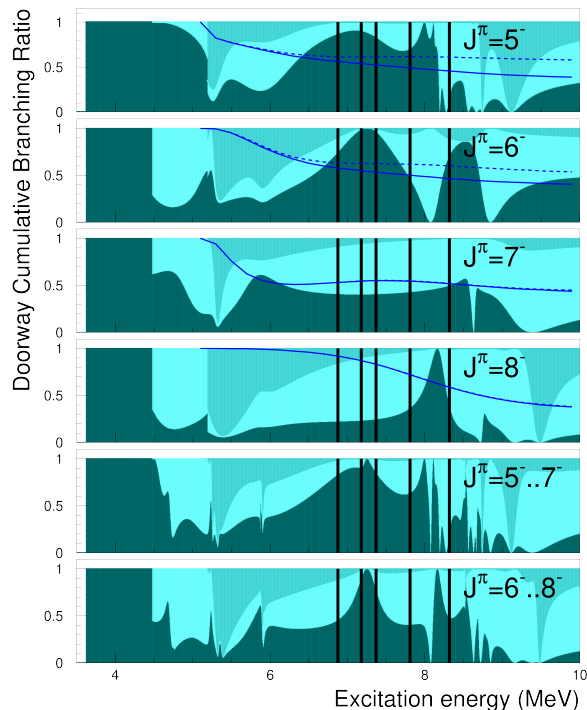

FIG. 5. A cumulative plot of calculated neutron branching ratios of $J^\pi = 5^-, 6^-, 7^-, 8^-$ ^{134}Sn states as a function of excitation energy with the doorway interpretation using neutron $L = 6$ emission from $0i_{13/2}$. The predictions of the Hauser-Feshbach model for a given spin are shown for comparison: solid blue line represents feeding to $7/2^-$ state and dashed blue line to $3/2^-$. The last two plots show average cumulative branching ratios expected in the Gamow-Teller decay for the ^{134}In ground state spins of $J^\pi = 6^-$ and $J^\pi = 7^-$, respectively.
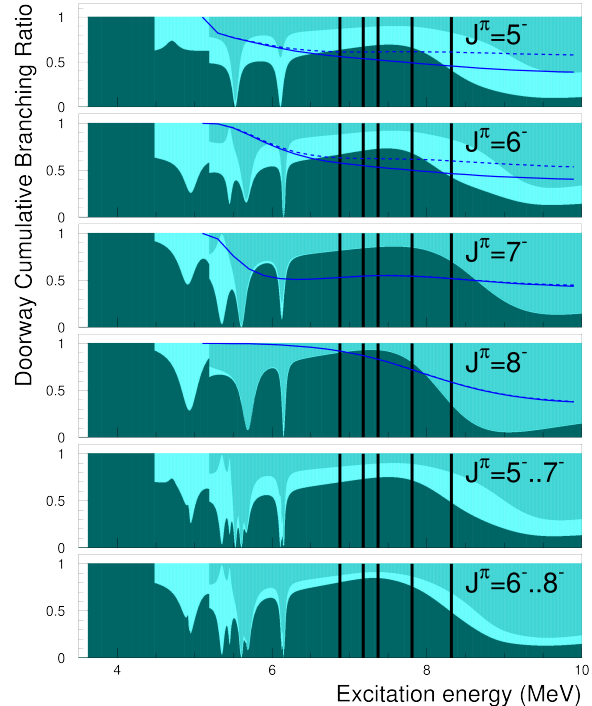

FIG. 6. Same as Fig. 5, except that the doorway interpretation uses $L = 4$ neutron emission from $1g_{9/2}$.

C. Doorway state decay model

The inability of accurately reproducing the observed βn branching ratios compels us to revise the validity of model assumptions in the case of ^{134}In. Because of the different p-h nature of states populated via GT transformations in ^{134}Sn and the single-particle states in ^{133}Sn, the spectroscopic overlap between ^{134}Sn* and ^{133}Sn$+n$ is minute. In a few cases, it has been shown experimentally that this causes βn states to be as narrow as below a few keV, e.g., in ^{133}Sn [33, 34] and ^{87}Br [7, 35]. Determination of this overlap is beyond the current accuracy of LSSM calculations [36]. This small spectroscopic overlap in very neutron-rich nuclei is the primary mechanism for trapping the GT state before it can decay [37]. Delayed neutron emission models assumed that this state "diffuses" into an equilibrated system (compound nucleus) which does not have a memory of the initial state in the limit of the high density of states [2, 5]. However, in the decay of near-shell-closure nuclei such as ^{134}In, equilibration may not be achieved due to low level densities, and the nucleus is forced to decay via an alternative path even if it has a very small probability. In that case, the concept of a doorway state may be invoked to describe neutron emission [37–39]. The observed GT states may coexist with tails of broad resonant states with configurations that have a strong neutron emission channel. The configuration mixing effects beyond the present shell-model

calculation capability may nevertheless enable neutron emission. The mixing of p-h states and resonant states in ^{134}Sn (which have large spectroscopic overlap with low-lying ^{133}Sn states) may lead to modulation of neutron emission branching ratios.

We present a new schematic model for the βn process of ^{134}In which captures shell structure effects by including spectroscopic factors between neutron-emitting states and the single-particle states in ^{133}Sn. The resonant ^{134}Sn states with neutron-particle configurations that possibly have strong neutron emission to ^{133}Sn states were calculated using a second LSSM outside a ^{120}Sr ($Z = 38$, $N = 82$) core. The valence model space consists of proton orbitals between $Z = 38$ and $Z = 82$ ($1p_{1/2}$, $0g_{9/2}$, $0g_{7/2}$, $1d_{5/2}$, $1d_{3/2}$, $2s_{1/2}$ and $0h_{11/2}$), and neutron orbitals between $N = 82$ and $N = 126$ ($0h_{9/2}$, $1f_{7/2}$, $1f_{5/2}$, $2p_{3/2}$, $2p_{1/2}$, and $0i_{13/2}$). The modified residual interactions $jj56pna$ were used. This valence space should reliably predict excited states in ^{134}Sn which undergo neutron emission, including all states with a closed $N = 82$ shell that have a non-vanishing overlap with ^{133}Sn single particle states. These calculations predict $\sim$40 keV level spacing around 7-MeV excitation energy in ^{134}Sn, a factor 3 to 8 larger than expected by the Gilbert-Cameron formula. The energy profiles of these resonances are represented by Breit-Wigner distributions.

$$\Psi_n\left(E\right) = \frac{1}{\pi} \frac{\left(\frac{\Gamma_n}{2}\right)}{(E_0 - E)^2 + \left(\frac{\Gamma_n}{2}\right)^2},$$

$$\Gamma_n = \sum_i \Gamma'_{n,i} = \sum_i \Gamma_{n,i} \frac{S_{n,i}}{S_n}. \tag{1}$$

Subscripts n identify specific neutron-emitting states in ^{134}Sn and subscripts i denote neutron feeding to a unique ^{133}Sn single particle state. The partial widths of each state, $\Gamma_{n,i}$, are calculated using a Koning-Delaroche optical potential [31]. Modified partial decay widths, Γ', are generated by scaling $\Gamma_{n,i}$ by the ratio of the spectroscopic factor, $S_{n,i}$, with respect to the full spectroscopic strength for that state, S_n. The total width of each state, Γ_n, is the sum of the modified partial widths, Γ'. Neutron emission branchings from each ^{134}Sn state as a function of energy are given by

$$I_{n,i}\left(E\right) = \Psi_n\left(E\right) \times \left(\frac{\Gamma'_{n,i}}{\Gamma_n}\right),$$

$$I_i\left(E\right) = \sum_n I_{n,i}\left(E\right). \tag{2}$$

The modified partial decay widths determine the neutron branching ratios on a state-by-state basis in ^{134}Sn. Feeding intensities to individual ^{133}Sn states, $I_{n,i}$, are aggregated from all neutron-emitting states as shown in the second line of Equation 2. Calculations of neutron branching ratios as a function of excitation energy using the model presented above can be seen in Fig. 5, The stacked, shaded histograms show the cumulative branching ratio to each ^{133}Sn state as a function of energy using

neutron feeding intensities given by Equation 2. Noticeable is the modulation of the branching ratios over small changes in excitation energy resulting from the presence of excited states in ^{134}Sn which have non-vanishing overlap with ^{133}Sn. This behavior is not reflected in the statistical model calculations in Figure 4. The proximity of the p-h states populated in the β decay of ^{134}In to any of these resonances can generate a neutron emission pathway with increased decay probability to a particular state in ^{133}Sn. Such a mechanism may explain the deviation from Hauser-Feshbach model predictions.

Close inspection of the energy distribution of the spectroscopic factors for neutron emitting states reveals that only states with the non-zero occupation of $\nu i_{13/2}$ orbital contribute. Large spectroscopic factors are predicted in the excitation energy range between 4 and 6 MeV in ^{134}Sn, see Fig. 5. The doorway states around $E^* = 7 MeV$ in the energy range of the states coinciding with those populated in the Gamow-Teller transition are characterized by much smaller spectroscopic factors, and they are formed by coupling to the proton excitations across Z=50 shell-closure. For those states, neutron emission is also mediated by the $i_{13/2}$ contribution, and their excitation energy in ^{134}Sn depends on the magnitude of the proton shell gap. Here a relatively small shell gap of 3 MeV was used. We have explored another possibility of the doorway state formation using simplified calculations using ^{132}Sn ($Z = 50$, $N = 82$) core and a variation of $jj56pna$ interactions that includes the orbitals across N=126 closed shell. The calculations, including $1g_9/2$, are shown in Fig. 6. This variant of $jj56pna$ interaction is implemented in a valence space with ^{132}Sn closed core consisting of proton orbitals ($0g_{7/2}$, $1d_{5/2}$, $1d_{3/2}$, $2s_{1/2}$ and $0h_{11/2}$), and neutron orbitals ($0h_{9/2}$, $1f_{7/2}$, $1f_{5/2}$, $2p_{3/2}$, $2p_{1/2}$, $0i_{13/2}$ and $1g_9/2$). Such limited configuration space enables only very schematic calculations because of a minimal degree of configuration mixing with orbitals across N=126. The chosen shell-gap is 4 MeV, consistent with the theoretically expected value [40]. This calculation can result in doorway states with large spectroscopic factors with L=4 neutron emission centered around 8 MeV. The results for neutron emission branching ratios are shown in Fig. 6. A similar broad distribution of doorway state stemming from $3d_{5/2}$ (L = 2) orbital can be generated using a similar approach.

These presented above shell-model calculations provide multiple plausible scenarios for generating doorway states affecting neutron emission probabilities from excited states in ^{134}Sn. These states have to be constructed with correct spin and parities and excitation energies to enable configuration mixing with the states populated in Gamow-Teller decays of ^{134}In and have a strong probability of neutron emission to excited single-particle states in ^{133}In. An accurate model aiming to describe this process directly would require a diagonalization in a larger configuration space than what was used here.

V. SUMMARY AND CONCLUSIONS

In conclusion, experimental evidence was found suggesting the βn of ^{134}In cannot be explained through a CN assumption. Measured neutron-emission branching ratios from the ^{134}Sn excited states to single-particle states in ^{133}Sn deviate from statistical-model predictions. To explain this effect, we propose a hypothesis that the formation of an equilibrated (compound) nucleus may not be achieved in the GT decay of ^{134}In due to the low level density in the excitation energy range. A schematic formalism which uses shell model spectroscopic factors was developed. β-delayed neutron emission mediated through persisting doorway states may be a more general feature of this process. It will affect a broader range of nuclei and be of importance for the r-process modeling. For most astrophysical r-process scenarios, participating nuclei cannot be directly measured, thus models must rely on robust theoretical predictions. A more complete neutron emission framework is needed to explain the emission process fully, especially for nuclei with low level densities. This is especially relevant for r-process waiting point nuclei near closed shells. The same effect may strongly influence multi-neutron emission probabilities (P_{xn}) [3]. Variations in P_{xn} which are presently not considered could drastically change isotopic abundance predictions of r-process models. Similar effects may also affect β-delayed proton emission [41] in medium- and heavy-mass nuclei. Future experiments should aim to explore a broader range of nuclei when they become available in new generation radioactive beam facilities. Modern theoretical approaches which include time dependent evolution of nuclear systems are being developed and they may provide a more complete description of the observed phenomenon.

ACKNOWLEDGMENTS

[1] P. G. Hansen and B. Jonson, "Beta-Delayed Particle Emission From Neutron-Rich Nuclei," in *Particle Emission from Nuclei*, Vol. 3, edited by D. N. Poenaru and M. S. Ivaşcu (CRC Press, 1989) pp. 157–201, 1st ed.

[2] T. Kawano, P. Möller, and W. B. Wilson, Phys. Rev. C **78**, 054601 (2008).

[3] R. Yokoyama, R. Grzywacz, B. C. Rasco, N. Brewer, K. P. Rykaczewski, I. Dillmann, J. L. Tain, S. Nishimura, D. S. Ahn, A. Algora, J. M. Allmond, J. Agramunt, H. Baba, S. Bae, C. G. Bruno, R. Caballero-Folch, F. Calvino, P. J. Coleman-Smith, G. Cortes, T. Davinson, C. Domingo-Pardo, A. Estrade, N. Fukuda, S. Go, C. J. Griffin, J. Ha, O. Hall, L. J. Harkness-Brennan, J. Heideman, T. Isobe, D. Kahl, M. Karny, T. Kawano, L. H. Khiem, T. T. King, G. G. Kiss, A. Korgul, S. Kubono, M. Labiche, I. Lazarus, J. Liang, J. Liu, G. Lorusso, M. Madurga, K. Matsui, K. Miernik, F. Montes, A. I. Morales, P. Morrall, N. Nepal, R. D. Page, V. H. Phong, M. Piersa, M. Prydderch, V. F. E. Pucknell, M. M. Rajabali, B. Rubio, Y. Saito, H. Sakurai, Y. Shimizu, J. Simpson, M. Singh, D. W. Stracener, T. Sumikama, R. Surman, H. Suzuki, H. Takeda, A. Tarifeño Saldivia, S. L. Thomas, A. Tolosa-Delgado, M. Wolińska-Cichocka, P. J. Woods, and X. X. Xu, Phys. Rev. C **100**, 031302 (2019).

[4] V. Weisskopf, "The Statistical Theory of Nuclear Reactions," in *Lecture series in nuclear physics (MDDC 1175)* (U. S. Govt. Print. Off., Washington, 1947) pp. 80–114.

[5] J. Hardy, B. Jonson, and P. Hansen, Nuclear Physics A **305**, 15 (1978).

[6] W. Hauser and H. Feshbach, Phys. Rev. **87**, 366 (1952).

[7] K.-L. Kratz, W. Rudolph, H. Ohm, H. Franz, M. Zendel, G. Herrmann, S. Prussin, F. Nuh, A. Shihab-Eldin, D. Slaughter, W. Halverson, and H. Klapdor, Nuclear Physics A **317**, 335 (1979).

[8] M. Mumpower, R. Surman, G. McLaughlin, and A. Aprahamian, Progress in Particle and Nuclear Physics **86**, 86 (2016).

[9] S. Shalev and G. Rudstam, Phys. Rev. Lett. **28**, 687 (1972).

[10] S. Prussin, Z. Oliveira, and K.-L. Kratz, Nuclear Physics A **321**, 396 (1979).

[11] C. E. Porter and R. G. Thomas, Phys. Rev. **104**, 483 (1956).

[12] P. Hoff, P. Baumann, A. Huck, A. Knipper, G. Walter, G. Marguier, B. Fogelberg, A. Lindroth, H. Mach, M. Sanchez-Vega, R. B. E. Taylor, P. Van Duppen, A. Jokinen, M. Lindroos, M. Ramdhane, W. Kurcewicz, B. Jonson, G. Nyman, Y. Jading, K.-L. Kratz, A. Wöhr, G. Løvhøiden, T. F. Thorsteinsen, and J. Blomqvist (ISOLDE Collaboration), Phys. Rev. Lett. **77**, 1020 (1996).

[13] M. Piersa-Siłkowska, A. Korgul, J. Benito, L. M. Fraile, E. Adamska, A. N. Andreyev, R. Álvarez-Rodríguez, A. E. Barzakh, G. Benzoni, T. Berry, M. J. G. Borge, M. Carmona, K. Chrysalidis, J. G. Correia, C. Costache, J. G. Cubiss, T. Day Goodacre, H. De Witte, D. V. Fedorov, V. N. Fedosseev, G. Fernández-Martínez, A. Fijałkowska, H. Fynbo, D. Galaviz, P. Galve, M. García-Díez, P. T. Greenlees, R. Grzywacz, L. J. Harkness-Brennan, C. Henrich, M. Huyse, P. Ibáñez, A. Illana, Z. Janas, K. Johnston, J. Jolie, D. S. Judson, V. Karanyonchev, M. Kicińska-Habior, J. Konki, L. Koszuk, J. Kurcewicz, I. Lazarus, R. Licǎ, A. López-Montes, H. Mach, M. Madurga, I. Marroquín, B. Marsh, M. C. Martínez, C. Mazzocchi, K. Miernik, C. Mihai, N. Mărginean, R. Mărginean, A. Negret, E. Nácher, J. Ojala, B. Olaizola, R. D. Page, J. Pakarinen, S. Pascu, S. V. Paulauskas, A. Perea, V. Pucknell, P. Rahkila, C. Raison, E. Rapisarda, K. Rezynkina, F. Rotaru, S. Rothe, K. P. Rykaczewski, J.-M. Régis, K. Schomacker, M. Siłkowski, G. Simpson, C. Sotty, L. Stan, M. Stǎnoiu, M. Stryjczyk, D. Sánchez-Parcerisa, V. Sánchez-Tembleque, O. Tengblad, A. Turturicǎ, J. M. Udías, P. Van Duppen, V. Vedia, A. Villa, S. Viñals, R. Wadsworth, W. B. Walters, N. Warr, and S. G. Wilkins (IDS Collaboration), Phys. Rev. C **104**, 044328 (2021).

[14] K. L. Jones, A. S. Adekola, D. W. Bardayan, J. C. Blackmon, K. Y. Chae, K. A. Chipps, J. A. Cizewski, L. Erikson, C. Harlin, R. Hatarik, R. Kapler, R. L. Kozub, J. F. Liang, R. Livesay, Z. Ma, B. H. Moazen, C. D. Nesaraja, F. M. Nunes, S. D. Pain, N. P. Patterson, D. Shapira, J. F. Shriner, M. S. Smith, T. P. Swan, and J. S. Thomas, Nature **465**, 454 (2010).

[15] W. Huang, M. Wang, F. Kondev, G. Audi, and S. Naimi, **45**, 030002 (2021).

[16] M. Wang, W. Huang, F. Kondev, G. Audi, and S. Naimi, **45**, 030003 (2021).

[17] I. N. Borzov, Phys. Rev. C **67**, 025802 (2003).

[18] Z. Y. Xu, M. Madurga, R. Grzywacz, T. T. King, A. Algora, A. N. Andreyev, J. Benito, T. Berry, M. J. G. Borge, C. Costache, H. D. Witte, A. Fijalkowska, L. M. Fraile, H. O. U. Fynbo, A. Gottardo, C. Halverson, L. J. Harkness-Brennan, J. Heideman, M. Huyse, A. Illana, L. Janiak, D. S. Judson, A. Korgul, T. Kurtukian-Nieto, I. Lazarus, R. Lica, R. Lozeva, N. Marginean, R. Marginean, C. Mazzocchi, C. Mihai, R. E. Mihai, A. I. Morales, R. D. Page, J. Pakarinen, M. Piersa-Siłkowska, Z. Podolyák, P. Sarriguren, M. Singh, C. Sotty, M. Stepaniuk, O. Tengblad, A. Turturica, P. V. Duppen, V. Vedia, S. Vinals, N. Warr, R. Yokoyama, and C. X. Yuan, "Beta-delayed neutron spectroscopy of ^{133}in," (2023), arXiv:2303.12173 [nucl-ex].

[19] R. Catherall *et al.*, Journal of Physics G: Nuclear and Particle Physics **44**, 094002 (2017).

[20] V. Fedosseev *et al.*, Journal of Physics G: Nuclear and Particle Physics **44**, 084006 (2017).

[21] W. A. Peters, S. Ilyushkin, M. Madurga, C. Matei, S. V. Paulauskas, R. K. Grzywacz, D. W. Bardayan, C. R. Brune, J. Allen, J. M. Allen, Z. Bergstrom, J. Blackmon, N. T. Brewer, J. A. Cizewski, P. Copp, M. E. Howard, R. Ikeyama, R. L. Kozub, B. Manning, T. N. Massey, M. Matos, E. Merino, P. D. O'Malley, F. Raiola, C. S. Reingold, F. Sarazin, I. Spassova, S. Taylor, and D. Walter, Nuclear Instruments and Methods in Physics Research Section A: Accelerators, Spectrometers, Detectors and Associated Equipment **836**, 122 (2016).

[22] S. V. Paulauskas, M. Madurga, R. Grzywacz, D. Miller, S. Padgett, and H. Tan, Nuclear Instruments and Methods in Physics Research Section A: Accelerators, Spectrometers, Detectors and Associated Equipment **737**, 22 (2014).

[23] J. Heideman, D. Pérez-Loureiro, R. Grzywacz, C. Thornsberry, J. Chan, L. Heilbronn, S. Neupane, K. Schmitt, M. Rajabali, A. Engelhardt, C. Howell, L. Mostella, J. Owens, S. Shadrick, E. Peters, A. Ramirez, S. Yates, and K. Vaigneur, Nuclear Instruments and Methods in Physics Research Section A: Accelerators, Spectrometers, Detectors and Associated Equipment **946**, 162528 (2019).

[24] H. Ohm, W. Rudolph, and K.-L. Kratz, Nuclear Physics A **274**, 45 (1976).

[25] S. Agostinelli, J. Allison, K. Amako, J. Apostolakis, H. Araujo, P. Arce, M. Asai, D. Axen, S. Banerjee, G. Barrand, F. Behner, L. Bellagamba, J. Boudreau, L. Broglia, A. Brunengo, H. Burkhardt, S. Chauvie, J. Chuma, R. Chytracek, G. Cooperman, G. Cosmo, P. Degtyarenko, A. Dell'Acqua, G. Depaola, D. Dietrich, R. Enami, A. Feliciello, C. Ferguson, H. Fesefeldt, G. Folger, F. Foppiano, A. Forti, S. Garelli, S. Giani, R. Giannitrapani, D. Gibin, J. Goméz-Cadenas, I. González, G. G. Abril, G. Greeniaus, W. Greiner, V. Grichine, A. Grossheim, S. Guatelli, P. Gumplinger, R. Hamatsu, K. Hashimoto, H. Hasui, A. Heikkinen, A. Howard, V. Ivanchenko, A. Johnson, F. Jones, J. Kallenbach, N. Kanaya, M. Kawabata, Y. Kawabata, M. Kawaguti, S. Kelner, P. Kent, A. Kimura, T. Kodama, R. Kokoulin, M. Kossov, H. Kurashige, E. Lamanna, T. Lampén, V. Lara, V. Lefebure, F. Lei, M. Liendl, W. Lockman, F. Longo, S. Magni, M. Maire, E. Medernach, K. Minamimoto, P. M. de Freitas, Y. Morita, K. Murakami, M. Nagamatu, R. Nartallo, P. Nieminen, T. Nishimura, K. Ohtsubo, M. Okamura,

S. O'Neale, Y. Oohata, K. Paech, J. Perl, A. Pfeiffer, M. Pia, F. Ranjard, A. Rybin, S. Sadilov, E. D. Salvo, G. Santin, T. Sasaki, N. Savvas, Y. Sawada, S. Scherer, S. Sei, V. Sirotenko, D. Smith, N. Starkov, H. Stoecker, J. Sulkimo, M. Takahata, S. Tanaka, E. Tcherniaev, E. S. Tehrani, M. Tropeano, P. Truscott, H. Uno, L. Urban, P. Urban, M. Verderi, A. Walkden, W. Wander, H. Weber, J. Wellisch, T. Wenaus, D. Williams, D. Wright, T. Yamada, H. Yoshida, and D. Zschiesche, Nuclear Instruments and Methods in Physics Research Section A: Accelerators, Spectrometers, Detectors and Associated Equipment **506**, 250 (2003).

[26] L. Carraz, P. Hansen, A. Huck, B. Jonson, G. Klotz, A. Knipper, K. Kratz, C. Miéhé, S. Mattsson, G. Nyman, H. Ohm, M. Poskanzer, A. Poves, H. Ravn, C. Richard-Serre, A. Schröder, G. Walter, and W. Ziegert, Physics Letters B **109**, 419 (1982).

[27] T. Otsuka, T. Suzuki, M. Honma, Y. Utsuno, N. Tsunoda, K. Tsukiyama, and M. Hjorth-Jensen, Phys. Rev. Lett. **104**, 012501 (2010).

[28] G. Bertsch, J. Borysowicz, H. McManus, and W. Love, Nuclear Physics A **284**, 399 (1977).

[29] S. Yoshida, Y. Utsuno, N. Shimizu, and T. Otsuka, Phys. Rev. C **97**, 054321 (2018).

[30] S. Okumura, T. Kawano, P. Jaffke, P. Talou, and S. Chiba, Journal of Nuclear Science and Technology **55**, 1009 (2018).

[31] A. Koning and J. Delaroche, Nuclear Physics A **713**, 231 (2003).

[32] F. D. Becchetti and G. W. Greenlees, Phys. Rev. **182**, 1190 (1969).

[33] V. Vaquero, A. Jungclaus, P. Doornenbal, K. Wimmer, A. Gargano, J. A. Tostevin, S. Chen, E. Nácher, E. Sahin, Y. Shiga, D. Steppenbeck, R. Taniuchi, Z. Y. Xu, T. Ando, H. Baba, F. L. B. Garrote, S. Franchoo, K. Hadynska-Klek, A. Kusoglu, J. Liu, T. Lokotko, S. Momiyama, T. Motobayashi, S. Nagamine, N. Nakatsuka, M. Niikura, R. Orlandi, T. Saito, H. Sakurai, P. A. Söderström, G. M. Tveten, Z. Vajta, and M. Yalcinkaya, Phys. Rev. Lett. **118**, 202502 (2017).

[34] M. Piersa, A. Korgul, L. M. Fraile, J. Benito, E. Adamska, A. N. Andreyev, R. Álvarez-Rodríguez, A. E. Barzakh, G. Benzoni, T. Berry, M. J. G. Borge, M. Carmona, K. Chrysalidis, J. G. Correia, C. Costache, J. G. Cubiss, T. Day Goodacre, H. De Witte, D. V. Fedorov, V. N. Fedosseev, G. Fernández-Martínez, A. Fijałkowska, M. Fila, H. Fynbo, D. Galaviz, P. T. Greenlees, R. Grzywacz, L. J. Harkness-Brennan, C. Henrich, M. Huyse, A. Illana, Z. Janas, K. Johnston, D. S. Judson, V. Karanyonchev, M. Kicińska-Habior, J. Konki, J. Kurcewicz, I. Lazarus, R. Lică, H. Mach, M. Madurga, I. Marroquín, B. Marsh, M. C. Martínez, C. Mazzocchi, N. Mărginean, R. Mărginean, K. Miernik, C. Mihai, E. Nácher, A. Negret, B. Olaizola, R. D. Page, S. Paulaskalas, S. Pascu, A. Perea, V. Pucknell, P. Rahkila, E. Rapisarda, J.-M. Régis, F. Rotaru, S. Rothe, V. Sánchez-Tembleque, G. Simpson, C. Sotty, L. Stan, M. Stănoiu, M. Stryjczyk, O. Tengblad, A. Turturica, J. M. Udías, P. Van Duppen, V. Vedia, A. Villa, S. Viñals, R. Wadsworth, W. B. Walters, and N. Warr (IDS Collaboration), Phys. Rev. C **99**, 024304 (2019).

[35] D. Slaughter, F. Nuh, A. Shihab-Eldin, and S. Prussin, Physics Letters B **38**, 22 (1972).

[36] A. Spyrou, S. N. Liddick, F. Naqvi, B. P. Crider, A. C. Dombos, D. L. Bleuel, B. A. Brown, A. Couture, L. Crespo Campo, M. Guttormsen, A. C. Larsen, R. Lewis, P. Möller, S. Mosby, M. R. Mumpower, G. Perdikakis, C. J. Prokop, T. Renstrøm, S. Siem, S. J. Quinn, and S. Valenta, Phys. Rev. Lett. **117**, 142701 (2016).

[37] N. Auerbach and V. Zelevinsky, Reports on Progress in Physics **74**, 106301 (2011).

[38] H. Feshbach, A. Kerman, and R. Lemmer, Annals of Physics **41**, 230 (1967).

[39] N. Auerbach and V. Zelevinsky, Nuclear Physics A **781**, 67 (2007).

[40] A. V. Afanasjev, S. E. Agbemava, D. Ray, and P. Ring, Phys. Rev. C **91**, 014324 (2015).

[41] J. C. Hardy and E. Hagberg, "Beta-Delayed Proton and Alpha Emission," in *Particle Emission from Nuclei*, Vol. 1, edited by D. N. Poenaru and M. S. Ivaşcu (CRC Press, 1989) pp. 99–131, 1st ed.